Small-angle neutron scattering by semicrystallized chains: evaluation of the mean dimensions

Jean Michel Guenet and Claude Picot
Centre de Recherches sur les Macromolécules, CNRS, 6 rue Boussingault, 67083 Strasbourg Cédex, France
(Received 12 December 1978)

The mean dimensions of semicrystallized chains having long crystallized sequences are calculated as functions of the crystallinity. Models of chain incorporated in the monocrystal are defined and their mean dimensions are expressed as functions of the molecular weight of the chain, taking into account the crystalline parameters. The effects of introducing amorphous sequences in the chain are then examined. Finally, the case of a real semicrystallized polymer containing pure amorphous regions is considered. The results are discussed as functions of crystallinity, molecular weight and crystalline parameters of two different polymers: polyethylene and isotactic polystyrene. In particular, it is shown that conformation with long crystallized sequences can lead to a non-variation of the radius of gyration as in Flory's model.

INTRODUCTION

Recent experiments have shown that the conformation of polymer chains in solution[1] or in the solid state[2,3] can be determined using the small-angle neutron scattering technique (SANS). The labelling of some chains by deuteration provides a neutron contrast without significantly changing the physicochemical properties of the polymers[4].

Many papers[2,3,5] have already been published on neutron scattering of amorphous as well as of crystallized polymers in the bulk state. In the latter case most experiments have been performed on polyethylene[5,6] for which fast crystallization processes occur in the medium. For polymers crystallized in bulk, the results have been interpreted using Flory's model for which the chain crystallizes through many monocrystals remaining globally Gaussian. We know of no calculations which evaluate the mean dimensions of conformations with long crystallized sequences. This situation could occur, for example, in monocrystals grown from dilute solutions[7,8] or in samples crystallized near the melting point and for polymers exhibiting slow growth in the rate of crystallization.

It is the purpose of this paper to determine the radii of gyration (which can be directly deduced from initial behaviour of the scattered intensity in SANS experiments) as functions of crystallinity taking into account that a crystalline polymer is generally an heterogenous medium. Two extreme idealized situations (*Figure 1*) can describe the heterogenity in our approach. The first (1) is a blend of amorphous chains on the one hand and fully crystallized chains confined to the same monocrystal on the other. In the second (2), chains made of long amorphous and crystalline sequences have the same crystallinity as the medium. To approach the chain conformation in a crystalline polymer these two extreme cases must be superposed. In such a frame, mean dimensions obtained in (1) and (2) have to be separately computed.

As a first step case (1) will be considered. Two different types of chain incorporation in the monocrystal have been then taken into account:

(i) unidirectional crystallization (UC). For this model (*Figure 2a*), the chain crystallizes along an (h, k, 0) plane of the crystalline lattice;

(ii) switch-board incorporation (SB). For this model the chain crystallizes always parallel to the c-axis of the crystalline lattice but otherwise unrestricted. This type of incorporation can be described with a two-dimension random walk (*Figure 2b*).

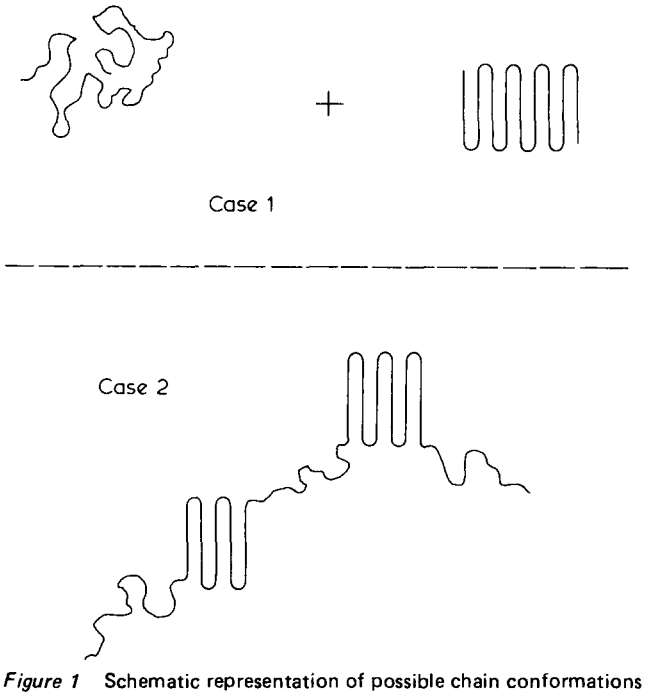

Figure 1 Schematic representation of possible chain conformations in a semicrystalline polymer

0032–3861/79/121473–10$02.00
© 1979 IPC Business Press

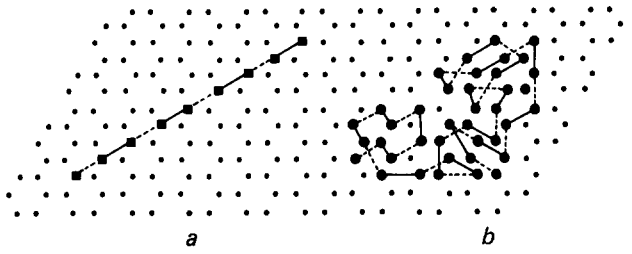

Figure 2 Schematic representation of an IPS monocrystal seen from above. Squares correspond to the UC incorporation while magnified points represent SB incorporation. Full lines and broken lines distinguish schematically the junction loops located on different sides of the monocrystal

As a second step, three models resulting from the combination of long crystallized and amorphous sequences (case 2 of *Figure 1*) are proposed (*Figure 3*):

(a) a model with one amorphous and one crystallized sequence (AC);

(b) a model with one crystallized and two amorphous sequences (ACA);

(c) a model with two crystallized and one amorphous sequence (CAC).

The results have been discussed in comparison with Gaussian statistics and Flory's model. They show that beyond three sequences Flory's behaviour is rapidly recovered, justifying our restriction.

General formulations have been developed introducing the molecular weight of the chain, its degree of crystallinity and the crystallographic parameters. Numerical calculations have been performed using either the parameters for polyethylene (PE) which has been widely studied or calculations which have been developed for isotactic polystyrene (IPS) for which experimental neutron scattering results are presented in the following paper.

THEORETICAL

The general expression of the apparent radius of gyration of a set of N scattering elements can be written:

$$\overline{R_g^2} = \frac{1}{\sum_i \sum_j \mu_i \mu_j} \sum_i \sum_j \mu_i \mu_j \overline{r_{ij}^2} \qquad (1)$$

where $\overline{r_{ij}^2}$ is the mean square distance between the scattering centres of contrast factor μ_i and μ_j.

For a tagged chain composed of two different scattering centres (in our case amorphous and crystalline sequences), the radius of gyration can be written according to an expression calculated by Leng and Benoit[9]:

$$\overline{R_g^2} = \left(\frac{\mu_c}{\mu}\right) \times \overline{R_c^2} + \left(\frac{\mu_a}{\mu}\right)(1-x)\overline{R_a^2} + \frac{\mu_c \mu_a}{\mu^2} \overline{L_G^2}(x)(1-x) \qquad (2)$$

for which μ_a, R_a and μ_c, R_c are respectively the contrast factors and the radii of gyration of amorphous and crystalline sequences, x is the crystallinity and $\overline{L_G^2}$ the mean square distance between the centres of mass of the two sequences. μ, μ_a, μ_c may be expressed as:

$$\mu = x\mu_c + (1-x)\mu_a$$

with

$$\mu_a = \bar{\nu}_a K_a'$$

and

$$\mu_c = \bar{\nu}_c K_c' \qquad (3)$$

where ν_a and ν_c are the specific volumes with self-explanatory subscripts and K_a' and K_c' depend only on the coherent lengths per unit volume of the monomer (b_m') and the surrounding (b_s') according to:

$$K' = b_m' - b_s' \qquad (4)$$

Since the monomer is the same for the two sequences, contrast factors μ_c and μ_a depend solely on the specific volumes. For many crystalline polymers, specific volumes differ by approximately 10%. From this argument it is easy to show that the terms $\mu_c x/\mu$ and $\mu_a(1-x)/\mu$ can be respectively approximated by x and $(1-x)$ without significantly changing the results. Finally, general expression of the radius of gyration useful in our study reduces to:

$$\overline{R_g^2} = \frac{1}{2N^2} \sum_i \sum_j \overline{r_{ij}^2} \qquad (5)$$

Chain crystallized in one monocrystal

We calculate expression (5) as a first step for the incorporation models UC and SB by considering *Figure 4*. The solid line represents the basic element needed for the calculation. By coupling several of these elements as in *Figure 4* both models may be built.

Let us consider two scattering centres of the crystallized chain belonging respectively to the basic elements i and j defined by their subscripts in and jm. The vector joining these two centres is:

$$\mathbf{r}_{in,jm} = \mathbf{r}_{in} + \mathbf{G}_i\mathbf{G}_j + \mathbf{r}_{jm} \qquad (6)$$

where $\mathbf{G}_i\mathbf{G}_j$ is the vector between the centres of mass of the two basic elements, $\mathbf{r}_{in}$ and $\mathbf{r}_{jm}$ are vectors joining the centre of mass of a basic element to one of its many scattering centres. The mean square distance becomes:

$$\overline{r_{in,jm}^2} = \overline{r_{in}^2} + \overline{G_iG_j^2} + \overline{r_{jm}^2} + \mathbf{G}_i\mathbf{G}_j \cdot \mathbf{r}_{in} + \mathbf{G}_i\mathbf{G}_j \cdot \mathbf{r}_{jm} + \mathbf{r}_{in} \cdot \mathbf{r}_{jm} \qquad (7)$$

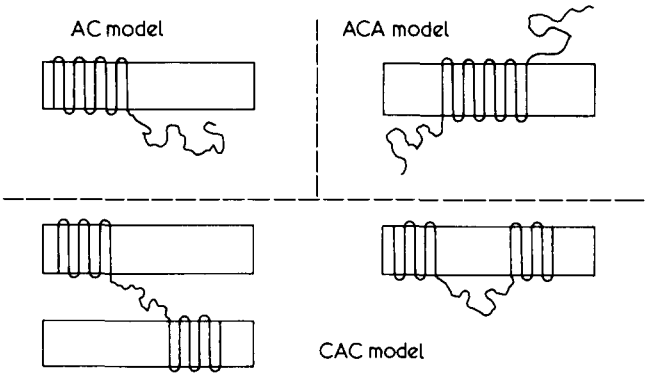

Figure 3 Models of crystallization involving large crystallized sequences

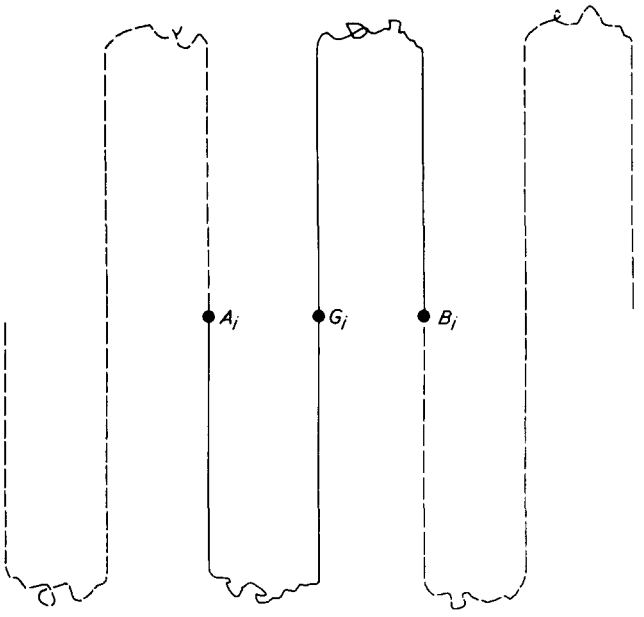

Figure 4 Representation of a basic element in a crystallized chain incorporated in the same monocrystal. G_i is the centre of mass

By summation and using the properties of the centre of mass, the three last terms in equation (7) vanish and the radius of gyration becomes:

$$R_g^2 = \frac{1}{2N_e^2 \cdot t^2} \sum_i \sum_j \sum_n \sum_m (\overline{r_{in}^2} + \overline{G_i G_j^2} + \overline{r_{jm}^2}) \quad (8)$$

where N_e is the number of basic elements and t the number of scattering centres in a basic element. Equation (8) becomes:

$$\overline{R_g^2} = \frac{1}{2N_e^2} \sum_i \sum_j \overline{G_i G_j^2} + \frac{1}{t} \sum_n \overline{r_n^2} \quad (9)$$

which can be written:

$$\overline{R_g^2} = \overline{R_p^2} + \overline{r_e^2} \quad (10)$$

for which $\overline{R_p^2}$ is a term depending on the mode of incorporation and $\overline{r_e^2}$ is the mean-square radius of gyration of the basic element. These two terms will now be calculated separately taking into account the incorporation models and the different conformation of the loops joining two consecutive rods.

Calculation of $\overline{r_e^2}$. For this purpose two simple cases are considered.

(i) *The conformation of the chain joining two consecutive rods is rod-like.*

Here we examine loops which are very tight and virtually rod-like. If k is the number of elements in a vertical rod and l in a horizontal rod-like loop, $\overline{r_e^2}$ can be written:

$$r_e^2 = \frac{1}{t} \left(2 \sum_1^{k/2} r_n^2 + 2 \sum_1^{l} r_n^2 + \sum_1^{k} r_n^2 \right) \quad (11)$$

Introducing $\overline{r_v^2}$, $\overline{r_b^2}$ the mean square radii of gyration of a vertical rod and of a rod-like loop, I the distance between two consecutive rods (which can be called the re-entry length) and $z = 2k/t$ ($1 - z = 2l/t$), we obtain:

$$\overline{r_e^2} = (3 - 2z)\overline{r_v^2} + 4(1 - z)\overline{r_b^2} + \frac{z}{2} \overline{I^2} \quad (12)$$

As the loop is rod-like $\overline{r_b^2} \sim \overline{I^2}/12$ leading to:

$$\overline{r_e^2} = (3 - 2z)\overline{r_v^2} + \frac{I^2}{6}(2 + z) \quad (13)$$

For the limiting cases $z = 0$ and $z = 1$ corresponding respectively to $\overline{r_v^2} = 0$ and $I = 0$ we find $\overline{r_e^2} = I^2/3$ and $\overline{r_e^2} = \overline{r_v^2}$ which shows the consistency of equation (13).

(ii) *The conformation of the chain joining two consecutive rods is statistical.*

In the case of statistical loops the extremities of which are separated by a distance I, the mean square radius of gyration is given by[10]:

$$\overline{r_b^2} = \frac{1}{12}(lb^2 + I^2) \quad (14)$$

with I and l as previously defined, and b^2 the mean-square length of the segments.

Expression (14) is valid in a first approximation where it is assumed that the chain conformation is not perturbed by the monocrystal surface. The calculation then yields:

$$\overline{r_e^2} = (3 - 2z)\overline{r_v^2} + 2(1 - z)\overline{r_b^2} + (2z + 1)\overline{I^2}/6 \quad (15)$$

For $z = 1$, we again obtain $\overline{r_e^2} = \overline{r_b^2}$ and for $\overline{r_b^2} \sim I^2/12$, equation (13) is also found.

Calculation of $\overline{R_p^2}$. We now calculate $\overline{R_p^2}$ for each of the two incorporation models.

(1) *Unidirectional crystallization (UC).* The distance D between two consecutive basic elements is:

$$D = 2I \quad (16)$$

Then:

$$\overline{R_p^2} = \frac{1}{2N_e^2} \sum_i \sum_j |i - j|^2 \cdot 4I^2 \quad (17)$$

which reduces to:

$$\overline{R_p^2} = N_p^2 (2I)^2/12 \quad (18)$$

Introducing the number of vertical rods, N_r, equation (18) becomes:

$$\overline{R_p^2} = N_r^2 I^2/12 \quad (19)$$

(2) *Switch-board implantation (SB).* As the trajectory of the chain is random, the basic element is no longer planar and is characterized by the angle Ψ defined between $\mathbf{G}_i\mathbf{B}_i$ and $\mathbf{A}_i\mathbf{G}_i$ (*Figure 4*). Simple geometrical and statistical considerations show that the mean value of Ψ is $\overline{\Psi} = \pi$. The problem reduces then to the previous case (planar basic ele-

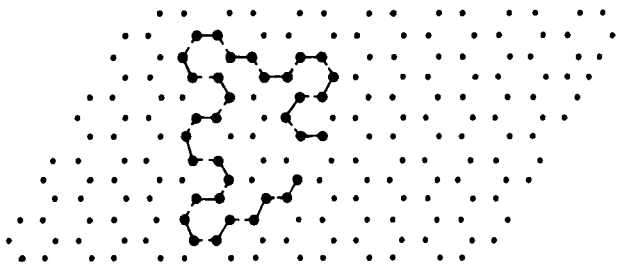

Figure 5 Schematic representation of a statistical adjacent re-entry (SAR) in an IPS monocrystal. Full and broken lines have the same significance as in *Figure 2*

ment), but the distance D between the centres of mass of two consecutive elements becomes $D = (2)^{1/2} I$ instead of $D = 2I$ for unidirectional crystallization. This must be also replaced in the r_e^2 relations. Now $\overline{R_p^2}$ can be calculated using the random walk calculation, which yields:

$$\overline{R_p^2} = N_r I^2/6 \tag{20}$$

Nevertheless this model is useful for re-entry lengths larger than the distance between two consecutive stems in the crystalline lattice. Thereby we have to consider the special case of statistical adjacent re-entry (SAR) which is also a two dimension incorporation but between nearest neighbour stems. It is then clear that the trajectory will be limited by the impossibility of 'crossing' itself (*Figure 5*). We are therefore dealing with a two dimensional self-avoiding walk. The exponent of the mean dimension can be calculated from a general expression given by De Gennes[1]:

$$\nu = \frac{3}{2+d} \tag{21}$$

where d is the dimensionality of the space which gives, for two dimensions, $\nu = 3/4$.

As in all the problems where we have to take into account excluded volume, the exact evaluation of $\overline{r_e^2}$ is not easy. By assuming a negligible contribution of the loops (rod-like 'loops') $\overline{R_p^2}$ can be expressed as:

$$R_p^2 = N_r^{1.5}\, I^2/8.75 \tag{22}$$

where 8.75 is obtained from $(1 + 2\nu)(2 + 2\nu)$[11].

To summarize all these results, we can put $\overline{R_p^2}$ in the general form:

$$R_p^2 = z^{2\nu} \left(\frac{M}{M_r}\right)^{2\nu} \frac{\overline{l^2}}{(1+2\nu)(2+2\nu)} \tag{23}$$

where M is the molecular weight of the chain and M_r the molecular weight of the vertical rod deduced from the thickness of the monocrystal.

Knowing $\overline{R_p^2}$ and $\overline{r_e^2}$ the use of equation (10) gives $\overline{R_g^2}$ for a tagged chain as a function of molecular weight, crystalline parameters and the model adopted.

The statistical calculations involved in our models suppose that we are dealing with a large number of vertical rods in order to eliminate the fact that the chosen basic element leads even to N_r, and in order to reach asymptotical behaviour for $\overline{R_p^2}$. It is generally admitted that this behaviour is obtained for a number of elements around 30. In the case of PE or IPS, taking into account models with negligible loops and a lamella thickness of 160[12] and 100 Å [13] respectively, one is led to the following lower limits for molecular weight:

PE $M \sim 5 \times 10^4$

IPS $M \sim 1.5 \times 10^5$

If 50% loops are present in the conformation the previous values have to be multiplied by a factor of two. On the other hand the upper molecular weights easily available are:

PE $M \sim 4 \times 10^5$

IPS $M \sim 1.5 \times 10^6$

Clearly there is a large range of molecular weights for which the above analysis pertains.

Semicrystallized chains containing large amorphous sequences

In the previous section, the amorphous material has been located only in the loops joining two consecutive rods. Let us now consider models with long crystallized and amorphous sequences. In this section the three different models presented in the Introduction are examined. The influence of the increase of the number of amorphous (A) and crystallized (C) sequences will be discussed afterwards.

AC model. This kind of model is similar to a diblock copolymer for which the radius of gyration has been already expressed by Leng and Benoit[9], namely:

$$\overline{R_g^2} = y\overline{R_{c,y}^2} + (1-y)\overline{R_{a,1-y}^2} + y(1-y)\overline{G_a G_c^2} \tag{24}$$

with y the weight fraction of chains in the crystallized sequence (including loops), $R_{c,y}^2$ and $R_{a,1-y}^2$ the radii of gyration of the crystallized and the amorphous sequences for given y, and $\overline{G_a G_c^2}$ the mean square distance between the centres of mass of the two sequences.

At first, $R_{c,y}$ and $R_{a,1-y}$ must be expressed as function of R_c and R_a which are, respectively, the radii of gyration for $y = 1$ and $y = 0$. If N_c is the number of monomers in the crystallized sequence and N_a in the amorphous one:

$$y = \frac{N_c}{N_a + N_c} \tag{25}$$

Assuming a Gaussian statistic $\overline{R_{a,1-y}^2}$ can be easily written:

$$\overline{R_{a,1-y}^2} = (1-y)R_a^2 \tag{26}$$

For $\overline{R_{c,y}^2}$ the three incorporation models defined previously must be considered. Then:

$$\overline{R_{c,y}^2} = \overline{R_{p,y}^2} + \overline{r_e^2} \tag{27}$$

leading finally to:

$$\overline{R_{c,y}^2} = y^{2\nu}\overline{R_p^2} + \overline{r_e^2} \tag{28}$$

with ν and $\overline{R_p^2}$ defined previously. Finally, $\overline{G_a G_c^2}$ expressions depending on the types of incorporation are obtained

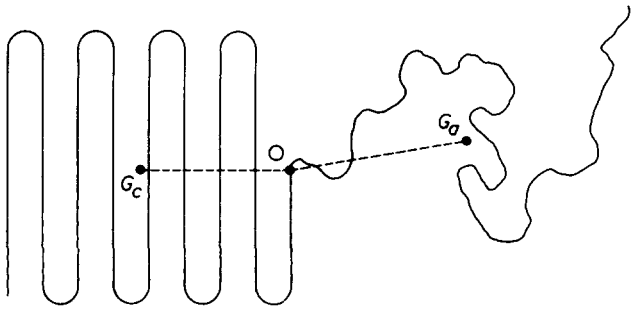

Figure 6 Schematic representation of the AC model

from simple geometrical considerations. Considering *Figure 6* and assuming the independence of orientation between vectors $\mathbf{OG}_a$ and $\mathbf{OG}_c$ one is lead to:

$$\overline{G_aG_c^2} = \overline{OG_a^2} + \overline{OG_c^2} \tag{29}$$

According to Gaussian statistics we obtain:

$$\overline{OG_a^2} = 2\overline{R_{a,1-y}^2} = 2(1-y)\overline{R_a^2} \tag{30}$$

For $\overline{OG_c^2}$, in the case of unidirectional implantation we find:

$$\overline{OG_c^2} = \left(\frac{L}{2}\right)^2 \tag{31}$$

Using $\overline{L^2} = 12\overline{R_{p,y}^2}$ and introducing $\overline{R_a^2}$ and $\overline{R_c^2}$ we obtain:

$$\overline{G_aG_a^2} = 3y^2\overline{R_p^2} + 2(1-y)\overline{R_a^2} \tag{32}$$

In the cases of SB and SAR incorporation $\overline{OG_c^2}$ can be expressed as:

$$\overline{OG_c^2} = 2\overline{R_{p,y}^2} \tag{33}$$

This yields:

for SB

$$\overline{G_aG_c^2} = 2y\overline{R_p^2} + 2(1-y)\overline{R_a^2} \tag{34}$$

for SAR

$$\overline{G_aG_c^2} = 2y^{1.5}\overline{R_p^2} + 2(1-y)\overline{R_a^2} \tag{35}$$

Finally, for each incorporation model the following expressions are deduced.

UC incorporation:

$$\overline{R_g^2} = (4-3y)y^3\overline{R_p^2} + y\overline{r_e^2} + (1-y)^2(2y+1)\overline{R_a^2} \tag{36}$$

SB incorporation:

$$\overline{R_g^2} = (-2y+3)y^2\overline{R_p^2} + y\overline{r_e^2} + (1-y)^2(2y+1)\overline{R_a^2} \tag{37}$$

SAR incorporation:

$$\overline{R_g^2} = (-2y+3)y^{2.5}\overline{R_p^2} + y\overline{r_e^2} + (1-y)^2(2y+1)\overline{R_a^2} \tag{38}$$

Three sequence models: ACA and CAC. Considering conformations of equivalent double sequences the radius of gyration can be then written:

$$R_g^2 = \frac{1}{2(2N+n)^2}\sum_i\sum_j r_{ij}^2 \tag{39}$$

where $2N$ and n are respectively the number of segments in the double sequence (β) and in the single sequence (γ). R_g^2 can be developed:

$$\overline{R_g^2} = \frac{1}{2(2N+n)^2}\left[2\sum_i\sum_j \overline{R_{ij}^2} + \sum_i\sum_j \overline{r_{ij}^2} + 4\sum_i\sum_j \overline{L_{ij}^2} + 2\sum_i\sum_j \overline{l_{ij}^2}\right] \tag{40}$$

where $\overline{R_{ij}^2}$, $\overline{r_{ij}^2}$, $\overline{L_{ij}^2}$, $\overline{l_{ij}^2}$ are respectively the mean square distances between points belonging to sequences β, γ, β and γ, β and β. Then equation (40) can be applied to the two considered models.

(i) *ACA model.* Taking some precautions which are described in Appendix 1 and using the same kind of calculation as previously we obtain:

for UC incorporation:

$$\overline{R_g^2} = (3-2y)y^2R_p^2 + y\overline{r_e^2} + \frac{(1-y)^2}{2}(2+y)\overline{R_a^2} \tag{41}$$

for SB incorporation:

$$\overline{R_g^2} = \frac{(3-y^2)}{2}y\overline{R_p^2} + y\overline{r_e^2} + \frac{(1-y)^2}{2}(2+y)\overline{R_a^2} \tag{42}$$

for SAR incorporation:

$$\overline{R_g^2} = -(5y^2+14y+35)\frac{y^{1.5}}{16}\overline{R_p^2} + y\overline{r_e^2} + \frac{(1-y)^2}{2}(2+y)\overline{R_a^2} \tag{43}$$

with $\overline{R_{c,y}^2} = y^{2\nu}\overline{R_p^2} + \overline{r_e^2}$ and $\overline{R_{a,1-y}^2} = (1-y)\overline{R_a^2}/2$

(ii) *CAC model.* This model involves two crystalline sequences. Structural studies, X-ray experiments in particular, show that consecutive crystalline lamellae are parallel. For this reason, the two different cases with crystalline sequences belonging or not to the same lamella have to be considered (see *Figure 3*). This last case clearly implies a correlation of orientation between crystallized blocks. Nevertheless, as explained in Appendix 2, a decorrelation of these orientations does not lead to different results.

Concerning the amorphous sequence in this model, it has been always considered Gaussian-like. This assumption could obviously become irrelevant for high degree of crystallinity.

Taking into account these considerations, we obtain:

for UC incorporation:

$$\overline{R_g^2} = \left(y^3 - \frac{3}{8}y^4\right)\overline{R_p^2} + y\overline{r_e^2} + \frac{(1-y)}{2}(-y^2+2y+2)\overline{R_a^2} \tag{44}$$

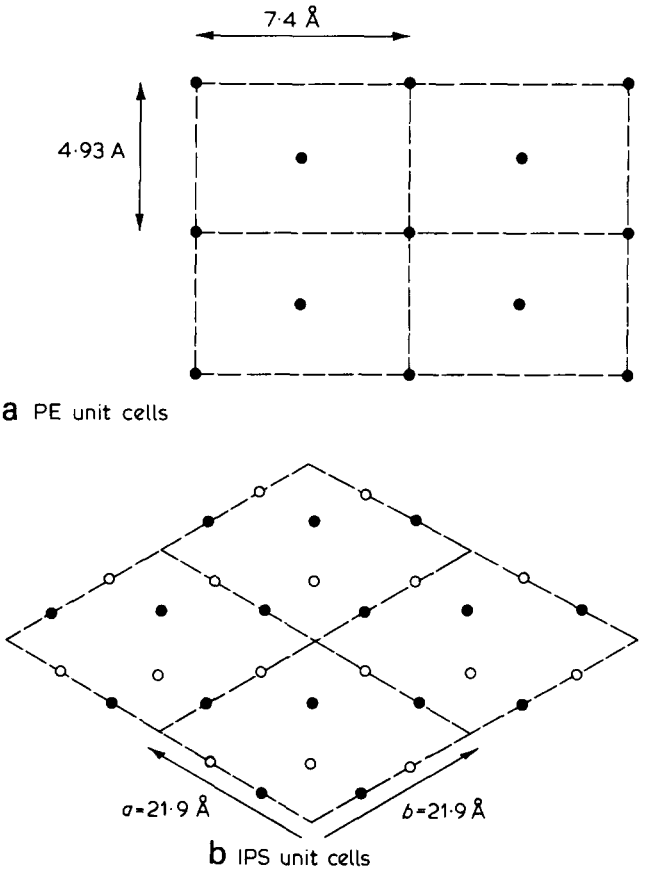

Figure 7 (a) Schematic representation of PE unit cells[14]; (b) Schematic representation of IPS unit cells[15]. Black points represent right-hand helix for instance and open circles left-hand helix

for SB incorporation:

$$\overline{R_g^2} = \left(-\frac{y^3}{4} + y^2\right)\overline{R_p^2} + y\overline{r_e^2} + \frac{(1-y)}{2}(-y^2 + 2y + 2)\overline{R_a^2} \tag{45}$$

for SAR incorporation:

$$\overline{R_g^2} = \left(\frac{y}{2}\right)^{1.5}(3y - y^2)\overline{R_p^2} + y\overline{r_e^2} + \frac{(1-y)}{2}(-y^2 + 2y + 2)\overline{R_a^2} \tag{46}$$

with, in that case

$$\overline{R_{c,y}^2} = \left(\frac{y}{2}\right)^{2\nu}\overline{R_p^2} + \overline{r_e^2}$$

and

$$\overline{R_{a,1-y}^2} = (1-y)\overline{R_a^2}$$

DISCUSSION

From all these relationships, it is clearly impossible to describe the specific behaviour of the different models. For this reason the calculations will be discussed and illustrated for IPS and PE as mentioned in the Introduction.

At first the mean dimensions of a tagged chain as function of the molecular weight for UC and SB incorporation modes will be examined. From these results AC, ACA and CAC models will be computed as a function of chain crystallinity. Finally, we will consider an heterogeneous system where the contribution of pure amorphous material has to be taken into account.

UC and SB models

In this section are presented numerical calculations of the radius of gyration as a function of molecular weight for chains confined to the same monocrystal. It must be noticed that such cases could occur in monocrystals grown from dilute solution. In *Figures 7a* and *7b* are drawn the unit cells of PE[14] and IPS[15]. From the *a* and *b* parameters, one can determine the re-entry length in UC incorporation following the plane of implantation in the crystalline lattice[16].

For PE, the calculated variations of R_g as function of the molecular weight M in the case of UC and SB incorporations with l_c = 160 Å are represented in *Figure 8*. From these curves, it can be noticed that in the common range of PE molecular weights, the values of R_g differ considerably from the asymptotic behaviour reached for extremely large molecular weights. This is due to the fact that $\overline{r_e^2}$ is not negligible in comparison with $\overline{R_p^2}$. On the other hand, by considering UC incorporation and an amount of 50% of loops the variation of $\overline{R_g^2}$ is very close to $M^{0.5}$ in the range $10^5 < M < 2.5 \times 10^5$. A similar result has been found by Sadler and Keller on PE monocrystals[17] grown from dilute solutions. Complementary experiments allow them to conclude that PE tagged chains are incorporated along the (110) plane in this situation. This effect is amplified for SB mode for which in some cases (l = 10 Å) R_g does not vary. Finally, we can remark that these calculated values are smaller than those measured by SANS in the molten state[18].

For IPS, three types of implantation have been studied, these are represented in *Figure 9* (l_c = 100 Å). The R_g variations relative to IPS exhibit similar behaviour as for PE with

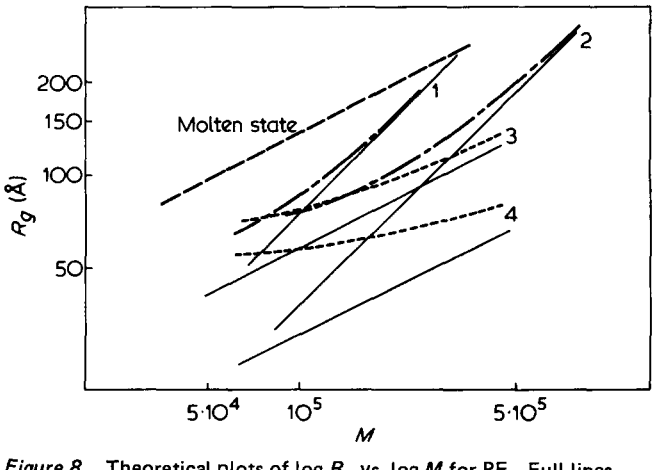

Figure 8 Theoretical plots of log R_g vs. log M for PE. Full lines give the value of $(\overline{R_p^2})^{1/2}$; — · — · —, lines UC incorporation modes; — — — —, lines SB incorporation modes and broken lines values measured in the molten state by SANS[18]. A, UC incorporation with rod-like junctions. In this case (110) plane has been chosen[16,17] leading to l = 4.45 Å. Rod-like loops have been considered to be of the same type as vertical rods in the calculation of $\overline{r_e^2}$. B, UC incorporation with 50% of loops. The radius of gyration of the loops has been obtained by using the relation $R = 0.45 \times M^{0.5}$ [18]. C and D are SB incorporation with respectively l = 20 Å and l = 10 Å, considering only rod-like junction

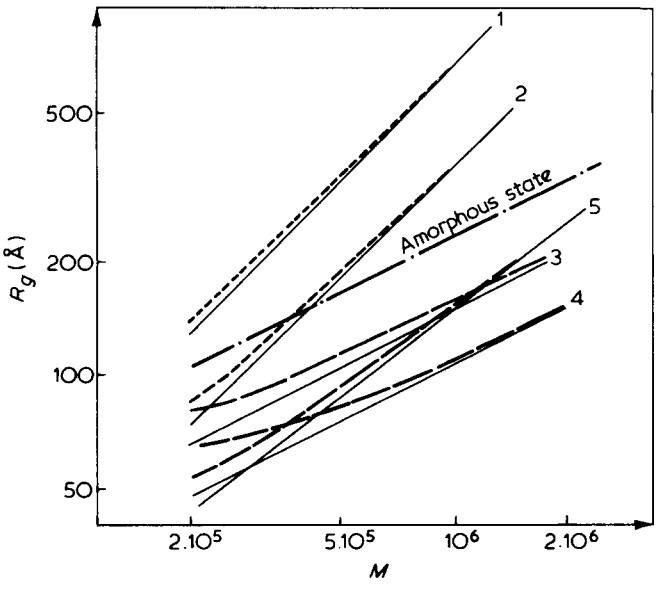

Figure 9 Theoretical plots log R_g vs. log M for IPS. Full lines give the $(\overline{R_0^2})^{1/2}$ values; - - - -, lines UC incorporation modes; — — —, lines SB modes and — · — · —, line values of R_g measured in the amorphous state[19] by SANS. A, UC incorporation with rod-like junctions. (110) plane has been chosen taking into account the most probable re-entrance of rods having same helical configuration[20]. This gives l = 12.6 Å. Rod-like junctions have been considered to be of the same type than vertical rods. B, UC incorporation with an amount of 50% loops. The radius of gyration of the loops has been determined from SANS measurements in the amorphous state[19]. C and D are SB incorporations with respectively l = 30 Å and l = 20 Å. Only rod-like junction models are represented; E, SAR incorporation with rod-like loops and l = 7.3 Å

the difference that the asymptotical behaviours are reached more rapidly. This results from the smaller values of the lamella thickness and the values of l which are higher in this polymer. The $\overline{r_e^2}$ term can be rapidly neglected for UC even by introducing 50% of loops. Lastly, contrarily to the PE, R_g variation for UC is located above the values obtained in the amorphous state while these for SB and SAR are below.

AC, ACA, CAC models

To illustrate the relations obtained for these models the radii of gyration of amorphous state given in refs 18 and 19 have been used again. Nevertheless, it has been shown by i.r. spectroscopy[16] that adjacent re-entry occurs preferentially along the (200) plane of the crystalline lattice for PE in the bulk crystallized state for which the models seem more adapted. Consequently, we will use the value l = 4.93 Å for the re-entry length concerning UC incorporation. In return, nothing will be changed to evaluate the radius of gyration for IPS in the crystalline state. The calculations are performed for each polymer for a single molecular weight which is chosen sufficiently high in order to use the relations in a large range of y, namely, PE M = 134 000, IPS M = 500 000, which correspond to the same number of monomer units for both polymers. $\overline{R_g^2}$ has been plotted as a function of y without introducing the effect of loops which will be examined further.

From the curves relative to PE (*Figure 10*) some comments can be made. Whatever the incorporation mode $\overline{R_g^2}$ decreases with y. For middle crystallinities (~50%) it looks difficult to appreciate a significant different between incorporation types.

For the CAC model and UC implantation $\overline{R_g^2}$ exhibits a very weak decrease with y.

However, two remarks arise from curves obtained for IPS (*Figure 11*). We observe very important differences in the variation of $\overline{R_g^2}$ for AC and ACA models between UC and SB types. The UC mode leads to an appreciable increase of $\overline{R_g^2}$ while $\overline{R_g^2}$ decreases with SB mode. Nevertheless, for CAC models with UC incorporation, $\overline{R_g^2}$ remains almost constant until y = 0.5. This degree of crystallinity cannot be usually exceeded for IPS. Then a certain ambiguity arises in the eventual choice between such a model and Flory's model. This also justifies the fact that calculations have not to be developed for an higher number of sequences to reach the non-variation of the radius of gyration.

These examples based on two different polymers describe the different behaviours related to the effect of the crystalline parameters. Thereby, it is clear that considerations proposed for PE cannot be necessarily applied to IPS or other polymers.

Heterogenous system: contribution of the amorphous material

Up to this point, only scattering from identical chains has been computed. As has been mentioned, blends of pure amorphous and semicrystallized chains must be considered. To describe such a system, a new set of parameters must be introduced, namely: w_a the weight fraction of chains in the amorphous continuum; w_c the weight fraction of amorphous chains located in the crystalline phase, and x, the weight

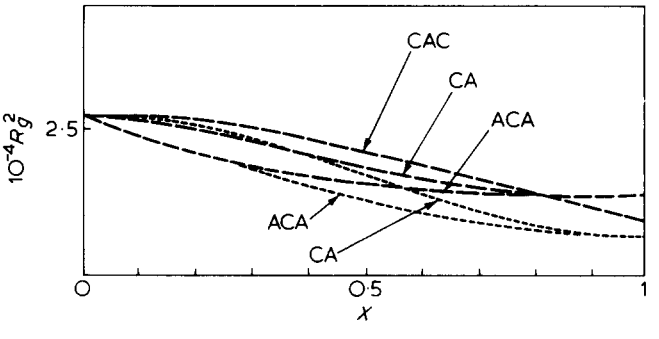

Figure 10 $\overline{R_g^2}$ as function of y for PE. — — —, lines represent UC incorporation and - - - - - - lines, SB incorporation

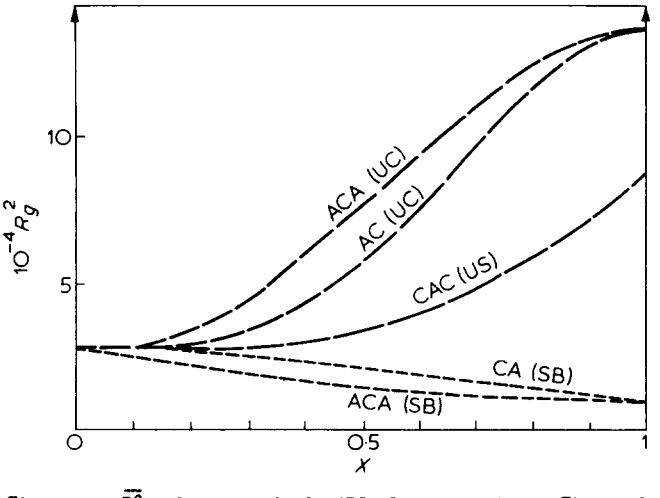

Figure 11 $\overline{R_g^2}$ as function of y for IPS. Same legend as in *Figure 10*.

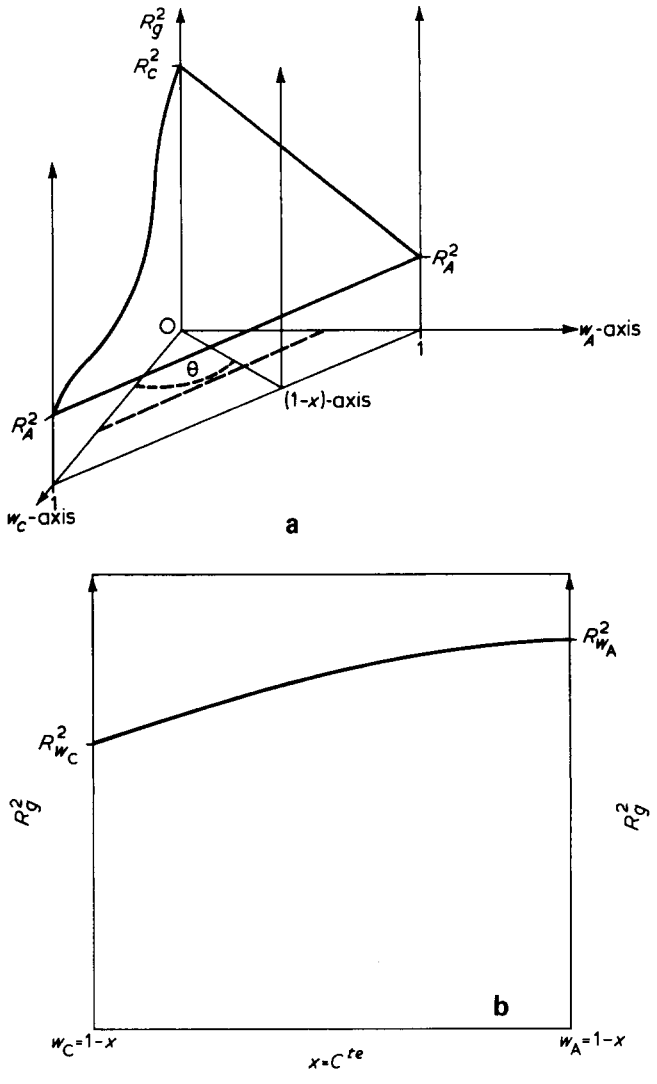

Figure 12 (a) Three dimensional diagram of $\bar{R}_g^2$ as function of w_a and w_c. One must notice that the scale on $(1-x)$-axis is not the same as that on w_a and w_c axes. The modulus ρ is given by

$$\rho = \frac{\sqrt{2}}{2} \frac{1}{(\cos \frac{\pi}{4} - \theta)}$$

so that the relation $w_a + w_c + x = 1$ is verified. (b) Representation of the variation of $\bar{R}_g^2$ as function of w_a and w_c at $x = C^{te}$

fraction of crystallized material (x is then the experimental crystallinity). As a first step the calculation will be restricted to $z = 1$(this means that loops defined previously are neglected). We then obtain the relations:

$$w_a + w_c + x = 1 \tag{47}$$

or

$$w_a + w_c = 1 - x \tag{48}$$

$\bar{R}_g^2$ clearly becomes:

$$\bar{R}_g^2 = w_a \bar{R}_a^2 + (w_c + x)\bar{R}^2_{w_c,x} \tag{49}$$

where $\bar{R}_a^2$ and $\bar{R}^2_{w_c,x}$ refer respectively to chains in the amorphous continuum and in the crystalline phase (note that $\bar{R}^2_{w_c,x}$ depends on R_a^2, R_p^2 and y with $y = x/x + w_c$, assuming that the mean dimensions of amorphous chains linked to crystalline sequences or dispersed in the amorphous surrounding do not differ significantly).

Such situations can be represented on a three dimensional diagram as in *Figure 12a*. The plane for $w_c = 0$ and $w_a = 0$ correspond respectively to cases 1 and 2 detailed in *Figure 1*. The angle θ is defined as $\tan\theta = w_a/w_c$. The dotted line (– – –) defines a plane for $x = C^{te}$. Such a plane is represented in *Figure 12b* where the variation of $\bar{R}_g^2$ is plotted for different repartitions of the amorphous material. This kind of representation is interesting since knowing experimental values of R_g and x one is then able to determine w_a and w_c for the different models. Thereby, the value of w_a can be compared with the experimental value deduced from other techniques.

To take the existence of loops into account, the same three-dimensional diagram can be drawn but the $(1-x)$-axis must be replaced by a $(1 - x/z)$-axis. Alternatively, for any w_a and w_c one will have:

$$y = \frac{x/z}{w_c + x/z} \tag{50}$$

Therefore $\bar{R}_g^2$ must be calculated according to:

$$\bar{R}_g^2 = W_a \bar{R}_a^2 + (w_c + x/z)\bar{R}^2_{w_c,x/z} \tag{51}$$

Another representation can be adopted for which curves obtained at $w_a = 0$ and $w_c = 0$ are plotted together. One then defines a domain in which the two extreme situations described in *Figure 1* are present. The chains fully incorporated in one monocrystal will have a radius of gyration given by equation (23). The loops will limit the crystallinity so that the maximum or minimum value of $\bar{R}_g^2$ will be given by (– · – · – line in *Figure 13*):

$$\bar{R}_g^2 = (xM/M_r)^{2\nu} \frac{I^2}{(1+2\nu)(2+2\nu)} + \bar{r}_e^2(x) \tag{52}$$

Using these considerations and different z parameters, a set of curves representing $\bar{R}_g^2$ as a function of x has been calculated (*Figure 13*) in the case of IPS for ACA model and

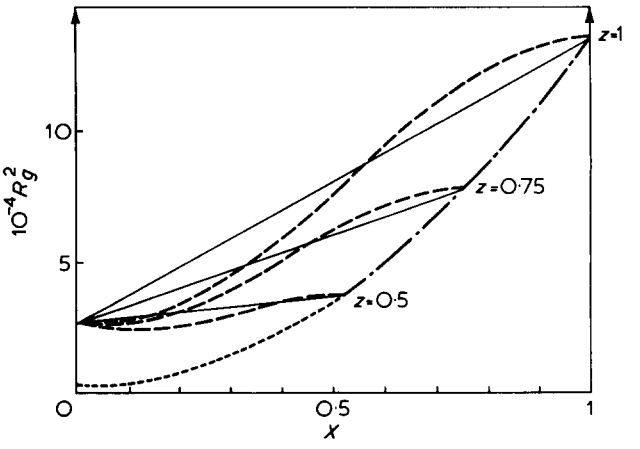

Figure 13 $\bar{R}_g^2$ vs x. Curves calculated for $w_a = 0$ (– – –) and $w_c = 0$ (———) are plotted on the same figure. The broken line (· – · –) is computed from equation (52) and gives the limit of $\bar{R}_g^2$ and x when loops are taken into account. For each value of z, a domain is defined in which chains having whether ACA, UC or amorphous conformations are blended for IPS

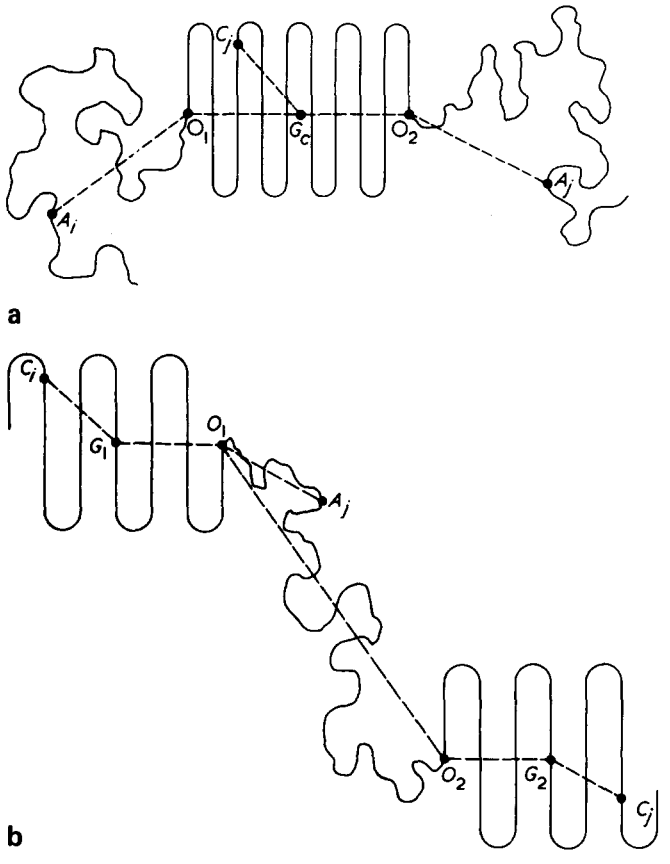

Figure 14 (a) Schematic representation of ACA model. (b) Schematic representation of CAC model

UC incorporation. However, this diagram is only useful as a first step in finding possible conformation. *Figure 13* points out that for an important loop contribution ($z \sim 0.5$) the mean dimensions are weakly affected by increasing crystallinity. This shows another example where the distinction between Flory's model and long crystallized sequences model (ACA) is ambiguous.

CONCLUSION

The models defined to perform these calculations may look somewhat primitive. However, they lead to expressions of the mean dimensions already delicate to handle. In a more accurate description of the conformations supplementary refinements should be introduced. For instance, conformation of amorphous loops and sequences in the crystalline phase has been assumed to be Gaussian and unperturbed by the vicinity of monocrystals. A better approximation should consist of taking into account the impossibility of the chain occupying the space delimited by the monocrystal. Alternatively a more realistic approach would envisage the possible polydispersity in composition leading to mean values of x and y.

Such calculations suppose that we are dealing with molecular weight monodisperse chains. It can be shown, especially in the case of UC incorporation that a measured radius of gyration in SANS must be associated with an average molecular weight given by:

$$M = \sqrt{M_z \cdot M_{z+1}}$$

Using M_w instead of this average in a plot $\log R_g$ vs. $\log M$ we are led to overestimate the values of R_g.

From R_g relations calculated in this paper, it appears that a single SANS experiment in the Guinier range does not always lead to an unambiguous determination of the crystalline chain conformation. Complementary information can be provided by studying the molecular weight dependence of R_g. Moreover, behaviour of the scattered intensity in the intermediate range of scattering vector could help to differentiate UC and SB incorporation modes. UC will correspond to a sheet (with $I(q) \sim q^{-2}$) while SB will correspond to a more compact medium (then $I(q) \sim q^{-n}$ with $n > 2$)[21].

APPENDIX

ACA model

We consider *Figure 14a*. $\mathbf{L}_{ij}$ defined in relation (40) can be expressed as:

$$\mathbf{L}_{ij} = \mathbf{A}_i\mathbf{C}_j = \mathbf{A}_i\mathbf{O}_1 + \mathbf{O}_1\mathbf{G}_c + \mathbf{G}_c\mathbf{C}_j \qquad \text{(A1)}$$

Then $\overline{L_{ij}^2}$ becomes:

$$\overline{L_{ij}^2} = \overline{A_iO_1^2} + \overline{O_1G_c^2} + \overline{G_cC_j^2} + 2\mathbf{A}_i\mathbf{O}_1\cdot\mathbf{O}_1\mathbf{G}_c + 2\mathbf{A}_i\mathbf{O}_1\cdot\mathbf{G}_c\mathbf{C}_j + 2\mathbf{O}_1\mathbf{G}_c\cdot\mathbf{G}_c\mathbf{C}_j \qquad \text{(A2)}$$

Assuming the decorrelation of orientation between $\mathbf{A}_i\mathbf{O}_1$ and $\mathbf{O}_1\mathbf{G}_c$, taking the summation over n and N and using the behaviour of the centre of mass, we finally obtain:

$$\sum_i^n \sum_j^N \overline{L_{ij}^2} = \sum_i^n \sum_j^N (\overline{A_iO_1^2} + \overline{O_1G_c^2} + \overline{G_cC_j^2}) \qquad \text{(A3)}$$

For $\mathbf{l}_{ij}$ defined in relation (40), we can also use the same kind of argument leading to:

$$\sum_i^N \sum_j^N \overline{l_{ij}^2} = \sum_i^N \sum_j^N (\overline{A_iO_1^2} + \overline{O_1O_2^2} + \overline{O_2A_j^2}) \qquad \text{(A4)}$$

From these relationships, which can be expressed as a function of $\overline{R_a^2}$, $\overline{R_p^2}$ and y we are able to calculate relations (41, 42, 43)

CAC model

Let us consider *Figure 14b*. Then $\mathbf{L}_{ij}$ can be written:

$$\mathbf{L}_{ij} = \mathbf{C}_i\mathbf{G}_1 + \mathbf{G}_1\mathbf{O}_1 + \mathbf{O}_1\mathbf{A}_j \qquad \text{(A5)}$$

By assuming the decorrelation of orientation between $\mathbf{G}_1\mathbf{O}_1$ and $\mathbf{O}_1\mathbf{A}_j$ and using the same arguments as previously, one obtains:

$$\sum_i^n \sum_j^N \overline{L_{ij}^2} = \sum_i^n \sum_j^N (\overline{C_iG_1^2} + \overline{G_1O_1^2} + \overline{O_1A_j^2}) \qquad \text{(A6)}$$

For $\mathbf{l}_{ij}$, we have:

$$\mathbf{l}_{ij} = \mathbf{C}_j\mathbf{G}_1 + \mathbf{G}_1\mathbf{O}_1 + \mathbf{O}_1\mathbf{O}_2 + \mathbf{O}_2\mathbf{G}_2 + \mathbf{G}_2\mathbf{C}_j \qquad \text{(A7)}$$

Considering that the angle ω between $\mathbf{O}_1\mathbf{G}_1$ and $\mathbf{O}_2\mathbf{G}_2$

can take all the values from 0 to 2π and using previous arguments, we finally deduce:

$$\sum_i^N \sum_j^N \overline{l_{ij}^2} = \sum_i^N \sum_j^N (\overline{C_j G_1^2} + \overline{G_1 O_1^2} + \overline{O_1 O_2^2} + \overline{O_2 G_2^2} + \overline{G_2 C_i^2}) \quad \text{(A8)}$$

It must be mentioned that in all these calculations we have not taken into account the effect of the monocrystal surface. Then the relations are only approximations which are not useful in the case of polymers having very large lamella thickness.

REFERENCES

1 Daoud, M. *et al. Macromolecules* 1975, **8**, 804
2 Kirste, R. G., Kruse, W. A. and Schelten, M. *Makromol. Chem.* 1972, **162**, 299
3 Cotton, J. P. *et al. Macromolecules* 1974, **7**, 863
4 Strazielle, C. and Benoit, H. *Macromolecules* 1975, **8**, 203
5 Schelten, J., Wignall, G. D. and Ballard, D. G. H. *Polymer* 1974, **15**, 682
6 Schelten, J. *et al. Polymer* 1977, **18**, 1111
7 Lotz, B., Kovacs, A. J., Bassett, G. A. and Keller, A. *Kolloid Z. Z. Polym.* 1966, **209**, 115
8 Sadler, D. M. and Keller, A. *Polymer* 1976, **17**, 37
9 Leng, M. and Benoit, H. *J. Polym. Sci.* 1962, **57**, 263
10 Levy, *Thesis* University of Strasbourg (1964)
11 Loucheux, C., Weil, G. and Benoit, H. *J. Chim. Phys.* 1958, *540*
12 Schelten, J., Ballard, D. G. H., Wignall, G. D., Longman, G. and Schmatz, W. *Polymer* 1976, **17**, 751
13 Overbergh, N., Berghmans, H. and Reynaers, H. *J. Polym. Sci.* 1976, **14**, 1177. The value of the lamella thickness considered is that measured for samples annealed around 185°C
14 Bunn, C. W. *Trans. Faraday. Soc.* 1939, **35**, 482
15 Natta, G. and Corradini, P. *Makromol. Chem.* 1955, **16**, 77
16 Bank, M. I. and Krimm, S. *J. Polym. Sci. (A-2)* 1969, **7**, 1785
17 Sadler, D. M. and Keller, A. *Macromolecules* 1977, **10**, 1128
18 Lieser, G., Fischer, E. W. and Ibel, K. *J. Polym. Sci.* 1975, 1313
19 Guenet, J. M., Picot, C. and Benoit, H. *Macromolecules* 1979, **12**, 86
20 Reiss, C. *J. Chim. Phys.* 1966, **10**, 1319
21 Yoon, D. Y. and Flory, P. J. *Polymer* 1977, **18**, 509